NACA

RESEARCH MEMORANDUM

EFFECT OF DESIGN OVER-ALL COMPRESSOR PRESSURE RATIO

DIVISION ON ACCELERATION CHARACTERISTICS OF THREE

HYPOTHETICAL TWO-SPOOL TURBOJET ENGINES

By Richard E. Filippi and James F. Dugan, Jr.

Lewis Flight Propulsion Laboratory
Cleveland, Ohio

CLASSIFICATION CHANGED

UNCLASSIFIED

To

NACA Res als   effective

By authority of VRN-126 ....Date...Au. 15, 1958

ΩMT 5-6-58   CLASSIFIED DOCUMENT

NATIONAL ADVISORY COMMITTEE
FOR AERONAUTICS
WASHINGTON
August 20, 1956

NATIONAL ADVISORY COMMITTEE FOR AERONAUTICS

RESEARCH MEMORANDUM

EFFECT OF DESIGN OVER-ALL COMPRESSOR PRESSURE RATIO

DIVISION ON ACCELERATION CHARACTERISTICS OF THREE

HYPOTHETICAL TWO-SPOOL TURBOJET ENGINES

By Richard E. Filippi and James F. Dugan, Jr.

SUMMARY

The effect of the design over-all compressor pressure ratio division on the acceleration characteristics of three hypothetical two-spool turbojet engines is analytically investigated. The design over-all total-pressure ratio of each engine is 12, and the design inner-turbine-inlet temperature is 2500° R at static sea-level conditions. The outer- and inner-compressor design pressure ratios, respectively, for the three engines are 2-6, 3-4, and 4-3. A constant-exhaust-nozzle-area acceleration from 40 to 100 percent design thrust is considered such that component operation is limited either by an inner-turbine-inlet temperature of 2800° R or by the stall-limit line of either compressor.

Increasing the inner-turbine-inlet temperature to initiate the acceleration resulted in the outer and inner compressors of each engine moving toward their stall-limit lines. The inner compressor was found to overspeed for all three engines investigated, but the amount of overspeed was small, the maximum being 1.7 percent for the engine with the 2-6 pressure ratio division. The transient-speed relation differed only slightly from the equilibrium-speed relation for the three engines investigated.

The acceleration times for the three engines were equal.

INTRODUCTION

In designing a two-spool turbojet engine with a particular over-all total-pressure ratio, the design pressure ratio division between the outer and inner compressors is a variable to be considered in the design analysis. It is possible that one pressure ratio division will have advantages over another regarding engine size and weight and equilibrium or transient performance.

        The effect of design pressure ratio division on two-spool turbojet-
engine equilibrium performance and component frontal areas is investigated
in reference 1. Each of the three hypothetical two-spool engines consid-
ered in reference 1 has a design over-all pressure ratio of 12. The divi-
sions of pressure ratio between the outer and inner compressors of the
three engines are 2-6, 3-4, and 4-3, respectively. On the basis of the
analysis of reference 1, it was concluded that one particular pressure
ratio division did not have any marked advantage regarding full-thrust
or cruise performance. The effect of pressure ratio division on the
frontal areas of the inlet, the combustor, the afterburner, and the ex-
haust nozzle for complete expansion was small. When one-stage turbines
were assigned to drive the outer and inner compressors, minimum turbine
frontal area was obtained by designing for an outer-compressor pressure
ratio less than the inner-compressor pressure ratio.

        The compressor and turbine operating trends during the acceleration
and deceleration of two hypothetical two-spool turbojet engines are dis-
cussed in reference 2. The two engines are characterized by the same
component performance maps, but the arbitrarily specified ratio of outer-
to inner-spool moment of inertia for one engine is 4 times that specified
for the other engine. For static sea-level operation and assigned values
of exhaust-nozzle area and inner-turbine-inlet temperature, transient
operating paths of the compressor and turbine components and the speed
variation of the outer and inner spools are found for the two engines.
The calculations indicate that the stall-limit line of the outer or the
inner compressor may be encountered during acceleration and that, for the
engine having the greater outer- to inner-spool moment-of-inertia ratio,
the stall-limit line of the outer compressor may be reached during de-
celeration. Increasing the ratio of outer- to inner-spool moment of in-
ertia by a factor of 4 resulted in an increase in the inner-spool over-
speeding from 0.4 to 2.2 percent at the end of the calculated acceleration.
The design values of inner- and outer-turbine equivalent specific work
were not exceeded during acceleration or deceleration.

        This report determines the effect of design pressure ratio division
on two-spool turbojet-engine accelerating characteristics. The three
hypothetical two-spool engines of reference 1 are investigated. Moment-
of-inertia values are calculated for each engine from generalized engine
data and engine geometry. At static sea-level conditions, each engine is
assumed to accelerate from 40 to 100 percent design thrust. During the
acceleration, the exhaust-nozzle area is held constant at its design value,
and operation is limited either by the compressor stall-limit line or by
a limiting inner-turbine-inlet temperature of 2800° R or 300° F higher than
design. The equilibrium and acceleration operating paths are located on
the compressor component maps by employing the equilibrium and transient
matching procedure discussed in references 3 and 2. The variations of
outer- and inner-compressor mechanical speed with time are shown to indi-
cate acceleration times and the amount of inner-compressor overspeeding.
The transient variation of inner- with outer-spool mechanical speeds is
also compared with the equilibrium variation for each engine.

SYMBOLS

A area, sq ft

a_{cr} critical velocity of sound, ft/sec

F thrust, lb

g standard gravitational acceleration, 32.2 ft/sec^2

H stagnation enthalpy, Btu/lb

J mechanical equivalent of heat, 778.2 ft-lb/Btu

N rotational speed, rpm

P total pressure, lb/sq ft

T total temperature, °R

U wheel speed, ft/sec

V velocity, ft/sec

w weight flow, lb/sec

δ ratio of total pressure to NACA standard sea-level pressure of 2116 lb/sq ft

θ ratio of total temperature to NACA standard sea-level temperature of 518.7° R

Subscripts:

h hub

i inner spool

o outer spool

x axial

1 outer-compressor inlet

2   outer-compressor exit, inner-compressor inlet

3   inner-compressor exit, combustor inlet

4   combustor exit, inner-turbine inlet

5   inner-turbine exit, outer-turbine inlet

6   outer-turbine exit

7   exhaust-nozzle exit

Compressor stations:

NR N^{th} rotor

NS N^{th} stator

METHOD OF ANALYSIS

Design Conditions

A cross section of a two-spool turbojet engine showing the location of the numerical stations is presented in figure 1. The three two-spool engines investigated in this report are designated as engines 26, 34, and 43. The first and last numerals of each designation represent the outer- and inner-compressor pressure ratios, respectively, for static sea-level operation. The static sea-level design conditions for all three engines are as follows:

Over-all compressor pressure ratio   12
Outer-compressor equivalent weight flow, lb/sec   150
Outer- and inner-compressor polytropic efficiencies, percent . . .   90
Inner-turbine-inlet temperature, ^{O}R   2500
Inner- and outer-turbine adiabatic efficiencies, percent   87

In order to operate at an inner-turbine-inlet temperature of 2500° R, turbine cooling is required. Air was chosen as the cooling medium and was considered to be bled from the exit of the inner compressor. For matching purposes, the cooling air required was assumed to be equal to the fuel added in the combustor. The cooling air was not returned to the main stream.

3993

3993

Component Performance

The compressor and turbine component maps for the three engines being investigated are the same as those in reference 1. Each compressor map was obtained by determining the backbone (the line of maximum adiabatic efficiency), the stall-limit line, and the constant-speed lines. The method and curves required to obtain the compressor over-all performance are presented in reference 1.

The turbine performance maps were obtained from the results of the experimental turbine reported in reference 4. Reference 1 discusses the method of obtaining the turbine performance maps.

Equilibrium Performance

Equilibrium engine performance at static sea-level conditions was obtained by matching the two-spool gas generator of each engine with a convergent nozzle. The equilibrium matching procedures of reference 3 were used to obtain gas-generator performance. The procedures and charts of reference 5 were used to find the thrust and exhaust-nozzle area at each match point. Isentropic flow was assumed downstream of the turbine exit.

For the design value of exhaust-nozzle area, the variation of inner- with outer-spool speed and the equilibrium paths on the outer- and inner- compressor maps were found from the static sea-level engine performance. To do this, values of T_4, $N_1/\sqrt{\theta_1}$, P_2/P_1, $w_1\sqrt{\theta_1}/\delta_1$, P_3/P_2, $w_1\sqrt{\theta_2}/\delta_2$, $N_i/\sqrt{\theta_2}$, and F were plotted against A_7 for constant values of $N_0/\sqrt{\theta_1}$. The design value of exhaust-nozzle area was read from the plot of T_4 against A_7 at the design values of T_4 and $N_0/\sqrt{\theta_1}$. The equilibrium-speed variation for the design value of A_7 was found from the plot of $N_i/\sqrt{\theta_1}$ against A_7 for constant values of $N_0/\sqrt{\theta_1}$. Equilibrium paths were plotted on the compressor maps for design exhaust-nozzle-area data read from the plots of P_2/P_1, $w_1\sqrt{\theta_1}/\delta_1$, P_3/P_2, and $w_1\sqrt{\theta_2}/\delta_2$ against A_7.

Transient Performance

Acceleration considered. - For each engine, a static sea-level acceleration from 40 to 100 percent design thrust is considered. During the acceleration, the exhaust-nozzle area is held constant at its design value, and operation is limited by the stall-limit line of either compressor or by a limiting inner-turbine-inlet temperature of 2800° R. Operation at the limiting temperature, which is 300° F higher than design, is assumed to be safe for short periods of time.

Two possible acceleration paths along which the outer compressor will operate are shown in figure 2. The acceleration path shown on the outer-compressor performance map in figure 2(a) is determined by operating the engine at the maximum allowable inner-turbine-inlet temperature of 2800° R throughout the acceleration. Figure 2(b) shows the acceleration path that would be obtained if the initial portion of the acceleration were limited by the compressor stall-limit line before the maximum inner-turbine-inlet temperature of 2800° R could be reached. Acceleration begins with each engine operating at its equilibrium condition for 40 percent design thrust. The outer-compressor equilibrium operating point corresponding to 40 percent design thrust is shown as point A in figure 2(a). An instantaneous increase in inner-turbine-inlet temperature at constant outer- and inner-spool mechanical speeds was assumed to initiate the acceleration. Inner-turbine-inlet temperature was increased to 2800° R, thus forcing the compressor to operate nearer its stall-limit line (point B). The excess torques acting on the outer and inner spools result in acceleration of both spools. The acceleration continued at a constant inner-turbine-inlet temperature of 2800° R until the outer-spool speed attained its design value (point C). The acceleration was assumed to terminate with an instantaneous decrease in inner-turbine-inlet temperature to 2500° R such that the outer compressor is operating at its design point (point D).

In figure 2(b) is shown the type of acceleration path that resulted if, upon initially increasing the inner-turbine-inlet temperature, the outer compressor operated at its stall-limit line before the inner-turbine limiting temperature of 2800° R could be reached. The inner-turbine-inlet temperature was, therefore, instantaneously increased to a value less than 2800° R at which the outer compressor operated at its stall-limit line (point A'). As the acceleration proceeded along the compressor stall-limit line, the inner-turbine-inlet temperature increased until the limiting value of 2800° R was obtained (point B). The acceleration then continued along the path BCD as previously described. The acceleration paths on the inner-compressor performance maps are similar to the paths on the outer-compressor performance maps.

Calculation procedure. - The compressor and turbine acceleration paths, the times required to accelerate, and the transient variations of inner- with outer-spool speed are calculated from the moment-of-inertia values, the compressor and turbine equilibrium performance maps, and the transient matching procedures that are discussed in detail in reference 2. The method used to calculate the values of outer- and inner-spool inertias is given in the appendix.

3993

At the beginning of the acceleration, the compressor and turbine op-
erating points are fixed by the assigned values of inner-turbine-inlet
temperature and exhaust-nozzle area and by the values of outer- and inner-
spool equivalent speed, which are assumed to be the equilibrium values at
40 percent design thrust. The accelerating torques on the outer and inner
spools are calculated from the component operating points. For a small
specified time interval, the increments in outer- and inner-spool speed
are calculated from the values of moment of inertia and accelerating torque.
The values of outer- and inner-spool speed at the end of the specified
time interval, together with the specified values of inner-turbine-inlet
temperature and exhaust-nozzle area, fix the component operating points
at the new time. The process is repeated until the design value of outer-
spool equivalent speed is attained. The time required to accelerate is
simply the sum of the individual small time intervals.

RESULTS AND DISCUSSION

Equilibrium and Transient Paths

The values of outer- and inner-spool moments of inertia as determined
in the appendix to obtain transient performance are as follows:

Engine	Inertia, lb-ft^2	
	Outer spool	Inner spool
26	106	317
34	181	242
43	242	181

The equilibrium and transient operating lines on the outer- and inner-
compressor performance maps are shown in figures 3 and 4, respectively,
from 40 to 100 percent design thrust for engines 26, 34, and 43. The
inner-turbine-inlet temperatures corresponding to the equilibrium point
at 40 percent design thrust are shown in the following table for the three
engines considered:

Engine	Temperature, T_4, °R
26	1640
34	1665
43	1680

Increasing the inner-turbine-inlet temperature from the equilibrium value moves the operating lines toward the outer- and inner-compressor stall-limit lines for all three engines. The stall-limit lines shown on the compressor performance maps are assumed to represent the limit of usable operation. Interaction effects between the outer and inner compressors on the compressor maps and their stall-limit lines were assumed to be negligible.

As may be seen in the outer-compressor performance map for engine 26 (fig. 3(a)), the transient operating line does not encounter the stall-limit line of the outer compressor during the acceleration. On approaching design speed the transient bends across the equilibrium operating line. Although the acceleration path which the outer compressor follows does not encounter the stall-limit line, the engine is not operating at the maximum allowable inner-turbine-inlet temperature of 2800° R during the initial portion of the acceleration. As will be shown on the inner-compressor performance map, the initial portion of the acceleration is limited by the inner-compressor stall-limit line.

Accelerating engine 34 from its equilibrium point results in operation on the outer-compressor stall-limit line only at the initial acceleration point (fig. 3(b)). With increasing speed, the transient operating line moves away from the stall-limit line toward the design point.

Instantaneously increasing the turbine-inlet temperature causes the outer compressor of engine 43 to operate at its stall-limit line, as seen in figure 3(c). The acceleration is limited by the stall-limit line up to approximately 80 percent outer-compressor equivalent speed. Above this speed the acceleration is restricted by the limiting inner-turbine-inlet temperature, and the operating line moves away from the stall-limit line.

The inner compressor of engine 26 operates along its stall-limit line during the first part of the acceleration (fig. 4(a)). Above approximately 87 percent inner-compressor equivalent speed, the inner turbine operates at 2800° R and the inner-compressor acceleration path approaches the equilibrium path. When the outer compressor reaches design speed, the inner compressor is overspeeding by approximately 2 percent design equivalent speed.

The transient operating lines located on the inner-compressor performance maps of engines 34 and 43 in figures 4(b) and (c), respectively, do not encounter the stall-limit line during any part of the transient. The bend in the inner-compressor acceleration path of engine 43 (fig. 4(c)) is caused by operation of the outer compressor along its stall-limit line during the first part of the acceleration, as shown in figure 3(c). For engines 34 and 43, the inner-spool equivalent speed is nearly equal to design equivalent speed when the outer compressor reaches design speed.

The turbine maps are not presented because the outer and inner turbines of the three engines investigated did not operate critically. During acceleration for all three engines, turbine limiting-loading was not reached. Design turbine equivalent specific work and design equivalent speed were not exceeded during the acceleration. A similar result is reported in reference 2, as mentioned previously, for two hypothetical engines investigated during acceleration at static sea-level conditions.

Acceleration Times and Inner-Compressor Overspeed

The times to reach the outer-compressor design point and the amount of inner-compressor mechanical overspeed when the outer compressor is at design speed are shown in figure 5. Outer- and inner-compressor mechanical speeds in percent design are plotted against time for the three engines investigated. Since the engines are investigated at static sea-level conditions, the outer-compressor mechanical speed is also the outer-compressor equivalent speed. Inner-compressor mechanical speed when the outer-compressor reaches design speed and acceleration times are shown in the following table:

Engine	Acceleration time, sec	Inner-compressor mechanical speed, percent design
26	1.5	101.7
34	1.5	100.5
43	1.5	100.5

For the three engines investigated it is apparent that the differences in inner-compressor overspeed are negligible, and acceleration times are equal.

Curves that show the deviation of the inner- and outer-spool mechanical-speed variation from equilibrium are referred to as "decoupling" curves. These curves are helpful in determining what type of control system will be utilized to achieve maximum thrust within safe operating conditions. If the inner-spool speed during a transient is found to be greater than its equilibrium value for a particular value of outer-spool speed, the inner spool is said to be leading the outer spool, or the outer spool lags the inner spool.

The variation of inner-compressor mechanical speed with outer-compressor mechanical speed is shown in figure 6 for equilibrium and transient operation. For each engine, the transient variation differs only slightly from the equilibrium variation. The decoupling curves (fig. 6) show that, as design speed is approached during the transient for the three engines investigated, the inner spool is leading the outer spool. Figures

6(a) and (b) show that the inner spool leads the outer spool for the full acceleration of engines 26 and 34. However, for engine 43, the inner spool lags the outer spool through most of the acceleration except near design speed, as shown in figure 6(c).

SUMMARY OF RESULTS

The following results were obtained from an analytical investigation to determine the effect of design pressure ratio division on the transient performance of three hypothetical two-spool engines. The three two-spool engines investigated are designated as engines 26, 34, and 43, the first and last numerals of each designation representing the outer- and inner-compressor pressure ratio, respectively. Each engine was accelerated from 40 to 100 percent design thrust at static sea-level conditions.

1. The acceleration times for the three engines were equal.

2. Increasing the inner-turbine-inlet temperature from the equilibrium value moved the operating lines toward the outer- and inner-compressor stall-limit lines for all three engines.

3. When the outer compressor reached its design equivalent speed, the inner compressor of each engine investigated was overspeeding, the maximum being 1.7 percent over design mechanical speed for engine 26.

4. The inner spool led the outer spool through the complete acceleration of engines 26 and 34, while for engine 43, the outer spool led the inner spool except near design speed. The transient-speed relation differed only slightly from the equilibrium-speed relation.

Lewis Flight Propulsion Laboratory
    National Advisory Committee for Aeronautics
        Cleveland, Ohio, April 16, 1956

APPENDIX - CALCULATION OF MOMENT OF INERTIA

Component geometry required for the inertia calculation was computed from specified variations of axial velocities, tip diffusion factor (ref. 6), and a blade tip solidity of 1.0 with compressor stage number and the following design values obtained from reference 1:

Air flow per unit frontal area at station 1, lb/(sec)(sq ft) . . . 35
Outer-compressor equivalent tip speed, ft/sec 1100
Outer-compressor inlet axial Mach number 0.6
Inner-compressor first-rotor tip relative Mach number 1.18
Inner- and outer-compressor-exit tangential velocity, ft/sec . . . 0
Inner-turbine-exit axial-velocity ratio, $V_{x,5}/a_{cr,5}$ 0.5
Number of inner-turbine stages 1
Inner-turbine loading parameter, $Jg(H_4 - H_5)/U_{h,5}^2$ 2.1
Outer-turbine-exit axial-velocity ratio, $V_{x,6}/a_{cr,6}$ 0.5
Number of outer-turbine stages 1
Outer-turbine loading parameter, $Jg(H_5 - H_6)/U_{h,6}^2$ 2.1

The axial-velocity variation used in this report to determine compressor geometry is shown in figure 7 as a plot of axial velocity against compressor axial station.

The assumed variation in compressor rotor tip diffusion factor against axial station is shown in figure 8. The number of compressor stages in the outer and inner spools of each engine was determined by assuming simple radial equilibrium and a free-vortex compressor design and by assigning tip diffusion factors and axial velocities stagewise through the compressor. Single-stage turbines were assigned to drive each compressor.

The compressor frontal area, which is the same for the three engines, was calculated from the compressor-inlet weight flow and weight flow per unit frontal area. In order to determine the frontal area of each turbine, the turbine-outlet conditions have to be calculated. The exit area of each turbine is calculated from the turbine-exit values of annular area and hub radius. Turbine-exit annular area is calculated from the turbine-exit design values of equivalent weight flow and axial-velocity ratio. Turbine-exit hub radius is found from the design values of loading parameter, turbine work, and rotational speed. The turbine frontal area was assumed equal to the turbine-exit area.

Two contemporary engines of different geometrical construction were analyzed to calculate the inertias of each rotating component. Their sum was then checked against the known engine inertia. Combining the information obtained, curves were drawn to allow a reasonable approximation of component inertias to be made with a variation in engine dimensions. Engine inertia was calculated from the sum of the compressor and turbine disc and blade inertias.

The resultant inertias as determined for the three hypothetical engines showed that the sums of all the component inertias for each engine were approximately equal. The difference between the maximum and the minimum calculated inertias with respect to the average was 5.3 percent. Therefore, the average inertia was taken to be the same for all the engines. This value was 423 pound-feet squared. It was also found that the ratio of the outer- to inner-spool inertia was approximately equal to the outer- to inner-compressor pressure ratio. Subsequently, the outer- and inner-spool inertias were apportioned according to the ratio of outer- to inner-compressor pressure ratio. The inertia values for each engine are listed in the section RESULTS AND DISCUSSION.

Inasmuch as the inertias for the hypothetical engines were determined from two engines having different geometrical construction, the final values are assumed to be representative and valid for comparative results.

REFERENCES

1. Dugan, James F., Jr.: Effect of Design Over-All Compressor Pressure Ratio Division on Two-Spool Turbojet-Engine Performance and Geometry. NACA RM E54F24a, 1954.

2. Dugan, James F., Jr.: Component Operating Trends During Acceleration and Deceleration of Two Hypothetical Two-Spool Turbojet Engines. NACA RM E54L28, 1955.

3. Dugan, James F., Jr.: Two-Spool Matching Procedures and Equilibrium Characteristics of a Two-Spool Turbojet Engine. NACA RM E54F09, 1954.

4. Heaton, Thomas R., Forrette, Robert E., and Holeski, Donald E.: Investigation of a High-Temperature Single-Stage Turbine Suitable for Air Cooling and Turbine Stator Adjustment. I - Design of Vortex Turbine and Performance with Stator at Design Setting. NACA RM E54C15, 1954.

5. Turner, L. Richard, Addie, Albert N., and Zimmerman, Richard H.: Charts for the Analysis of One-Dimensional Steady Compressible Flow. NACA TN 1419, 1948.

6. Lieblein, Seymour, Schwenk, Francis C., and Broderick, Robert L.: Diffusion Factor for Estimating Losses and Limiting Blade Loadings in Axial-Flow-Compressor Blade Elements. NACA RM E53D01, 1953.
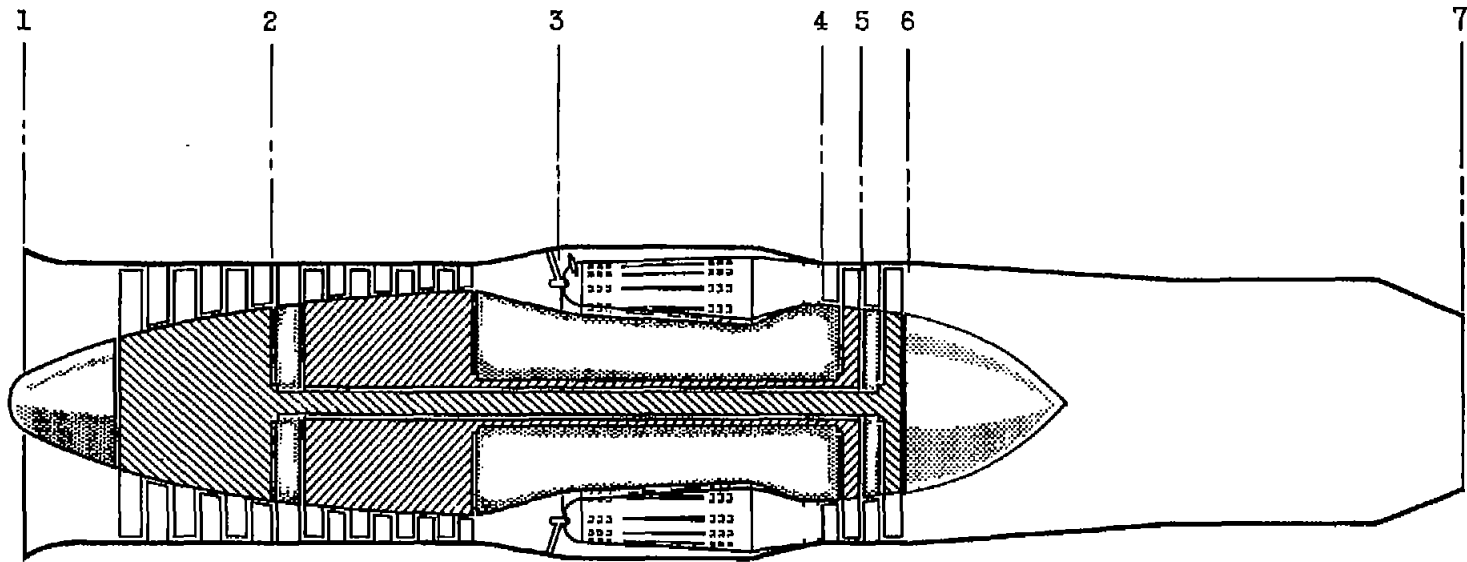
Figure 1. - Cross section of two-spool turbojet engine showing location of numerical stations.

Compressor-inlet equivalent weight flow, $w_1\sqrt{\theta_1}/\delta_1$, lb/sec
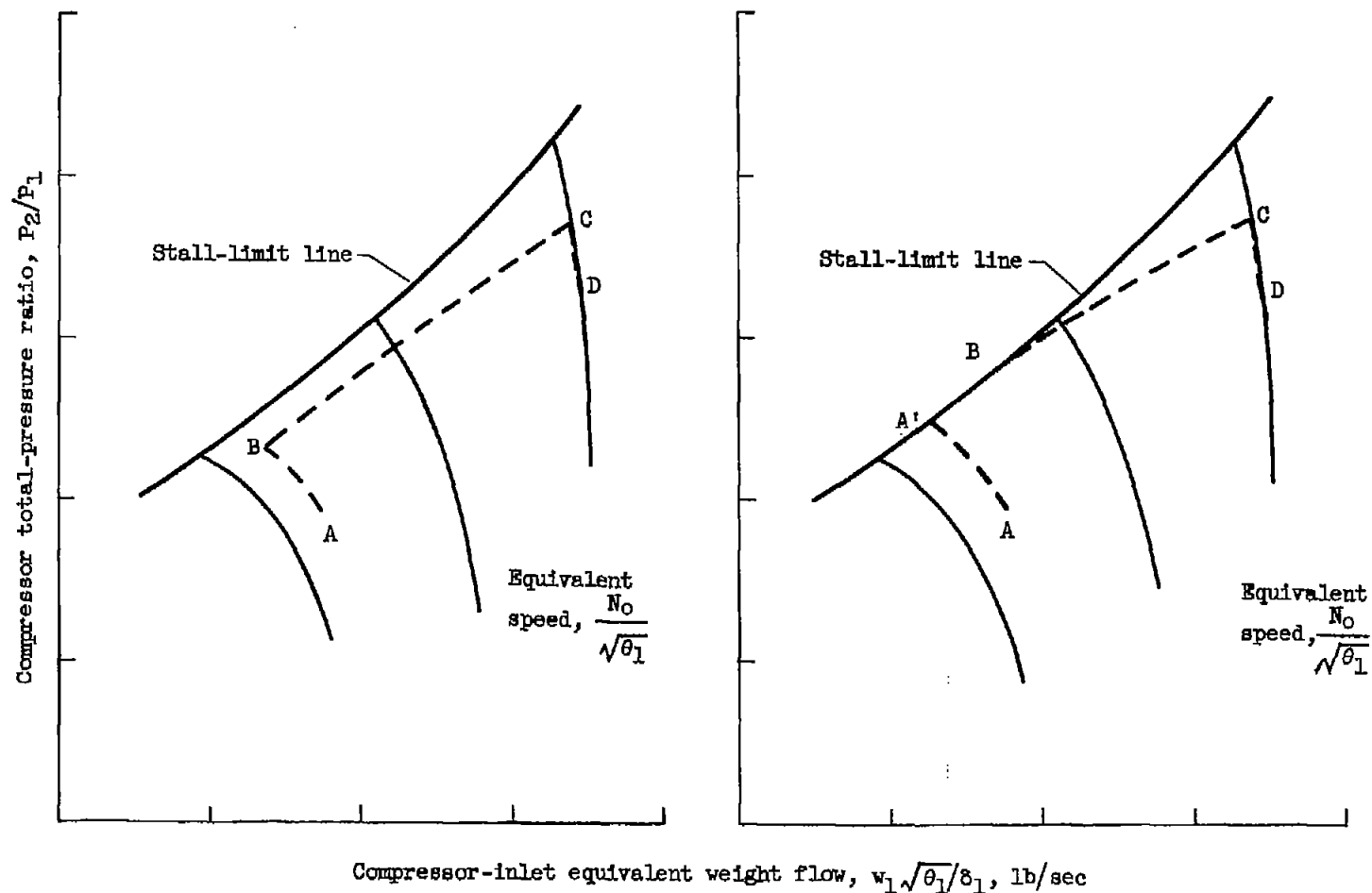
(a) Complete path limited by inner-turbine-inlet temperature.

(b) Path limited initially by stall-limit line and then by inner-turbine-inlet temperature.
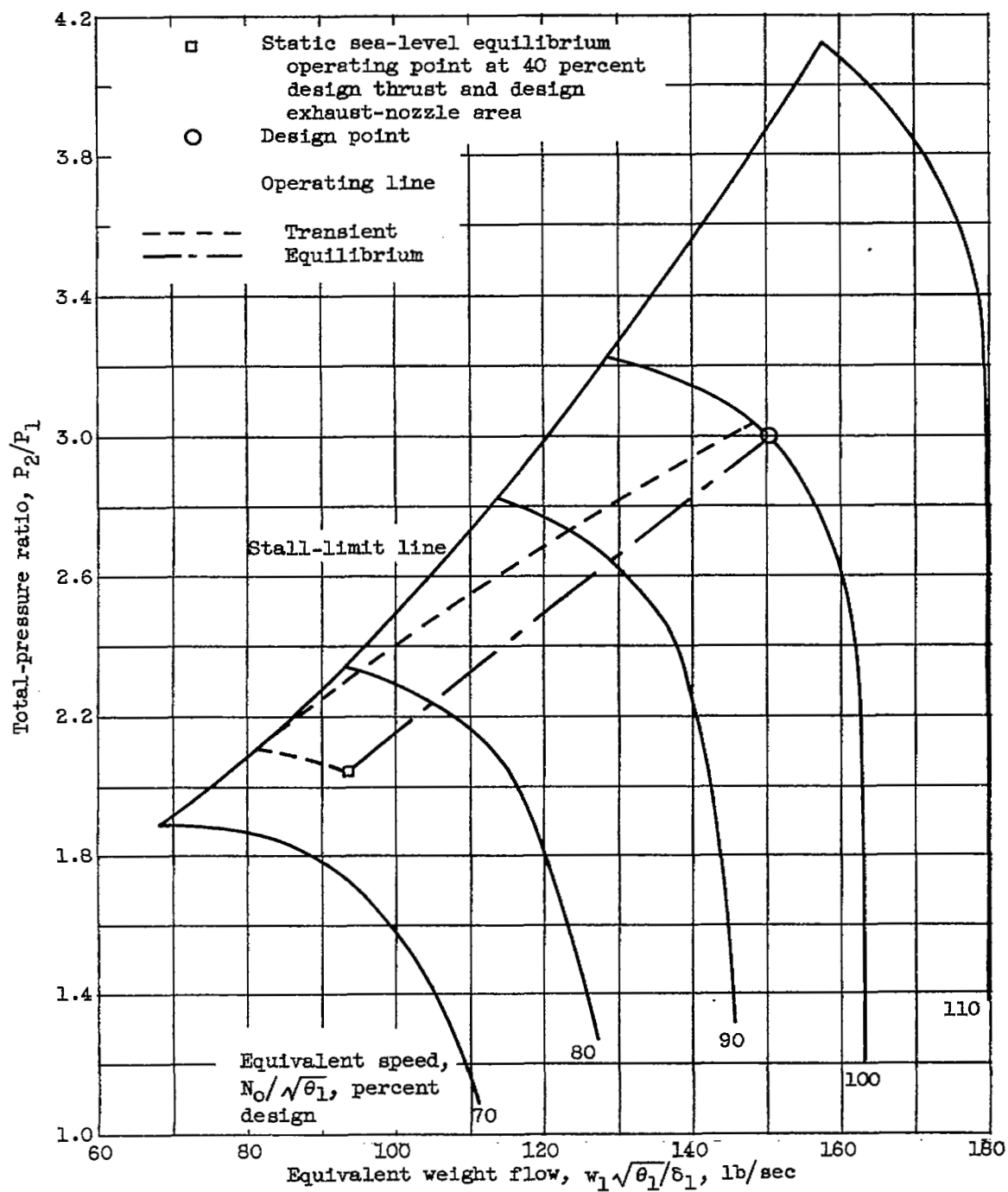
Figure 2. - Possible acceleration paths on outer-compressor performance map.
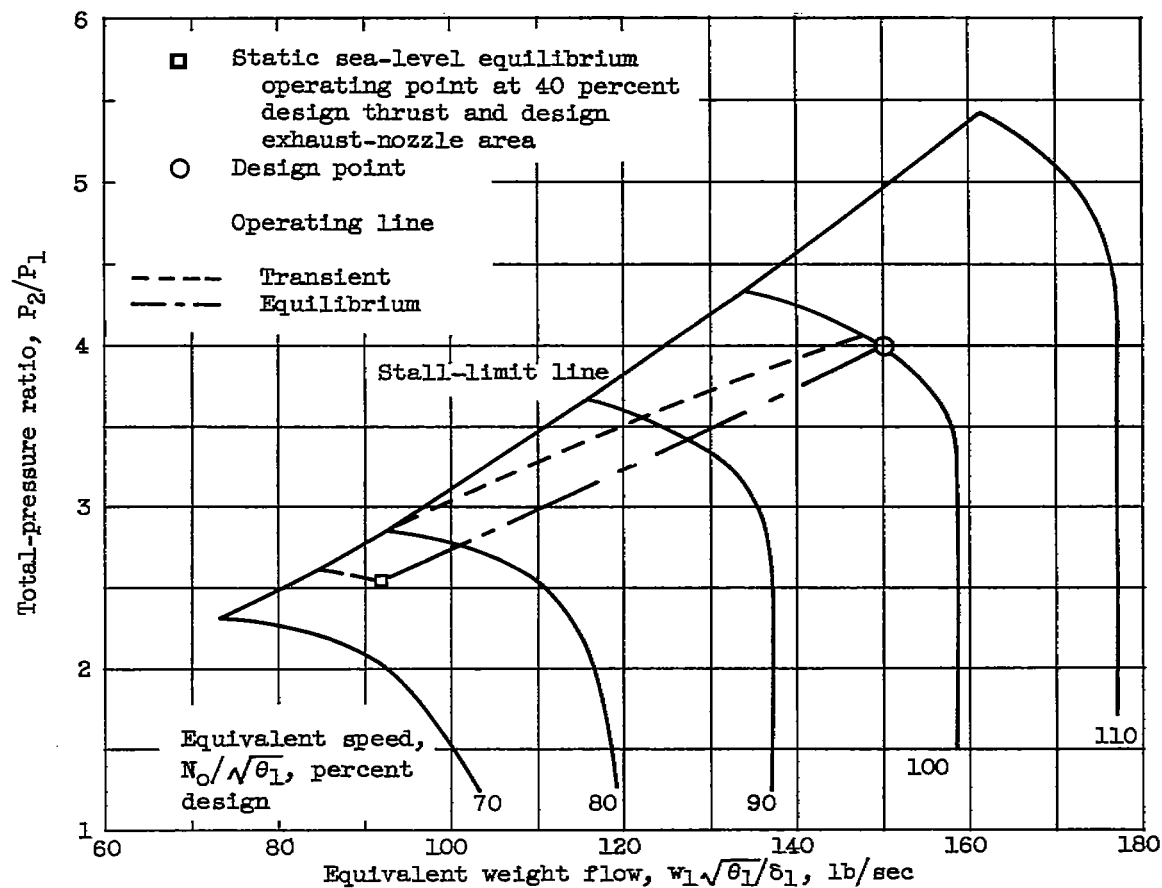
3993
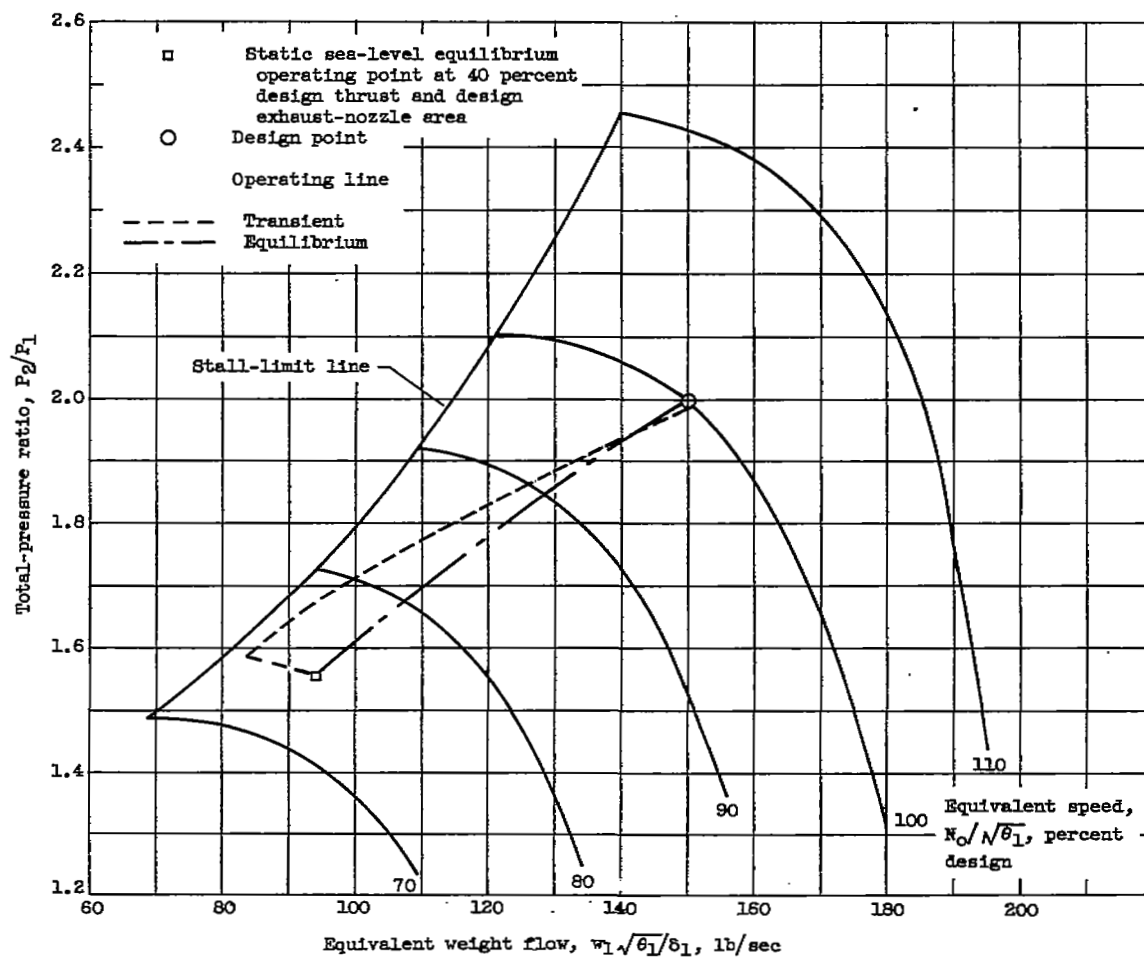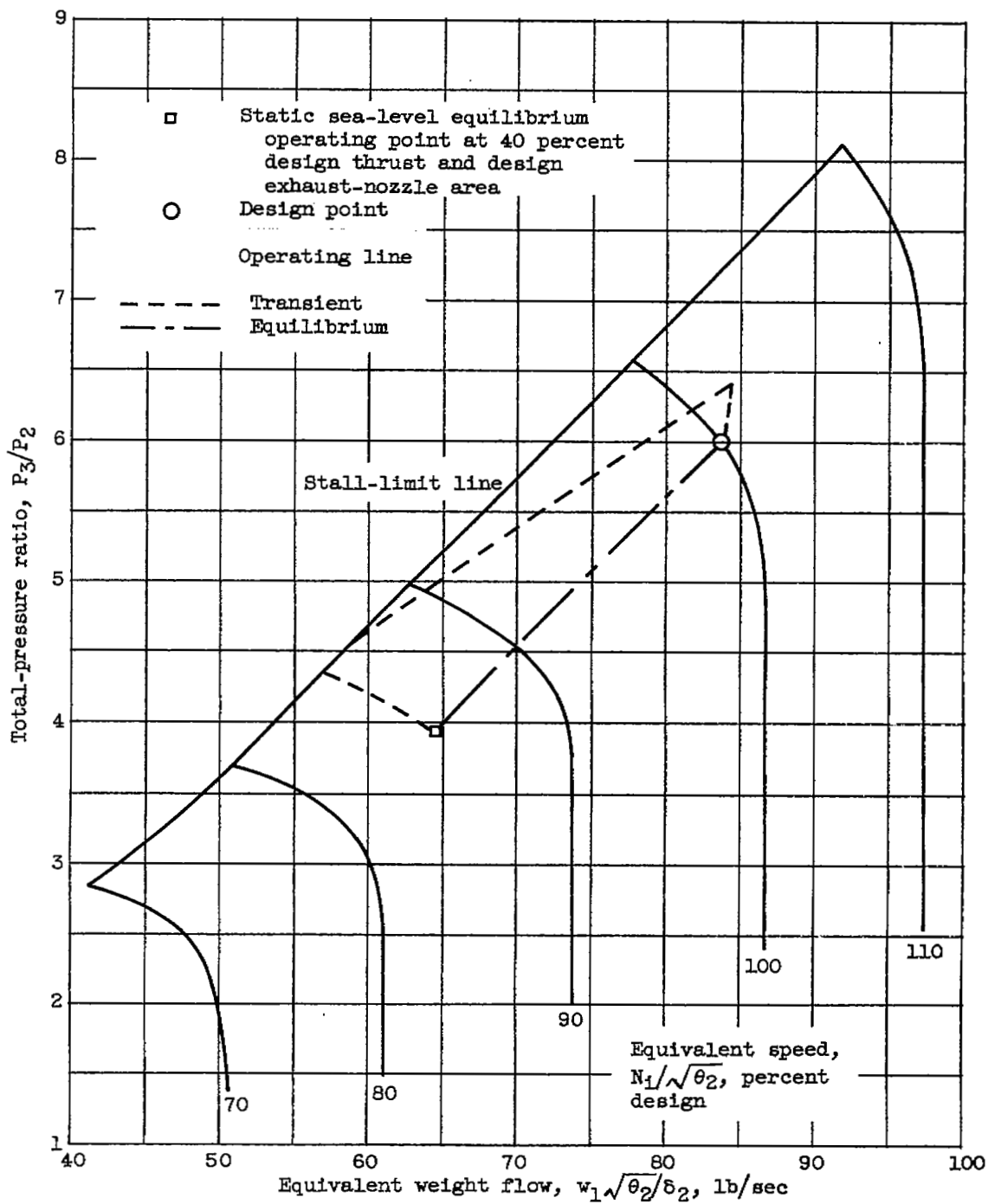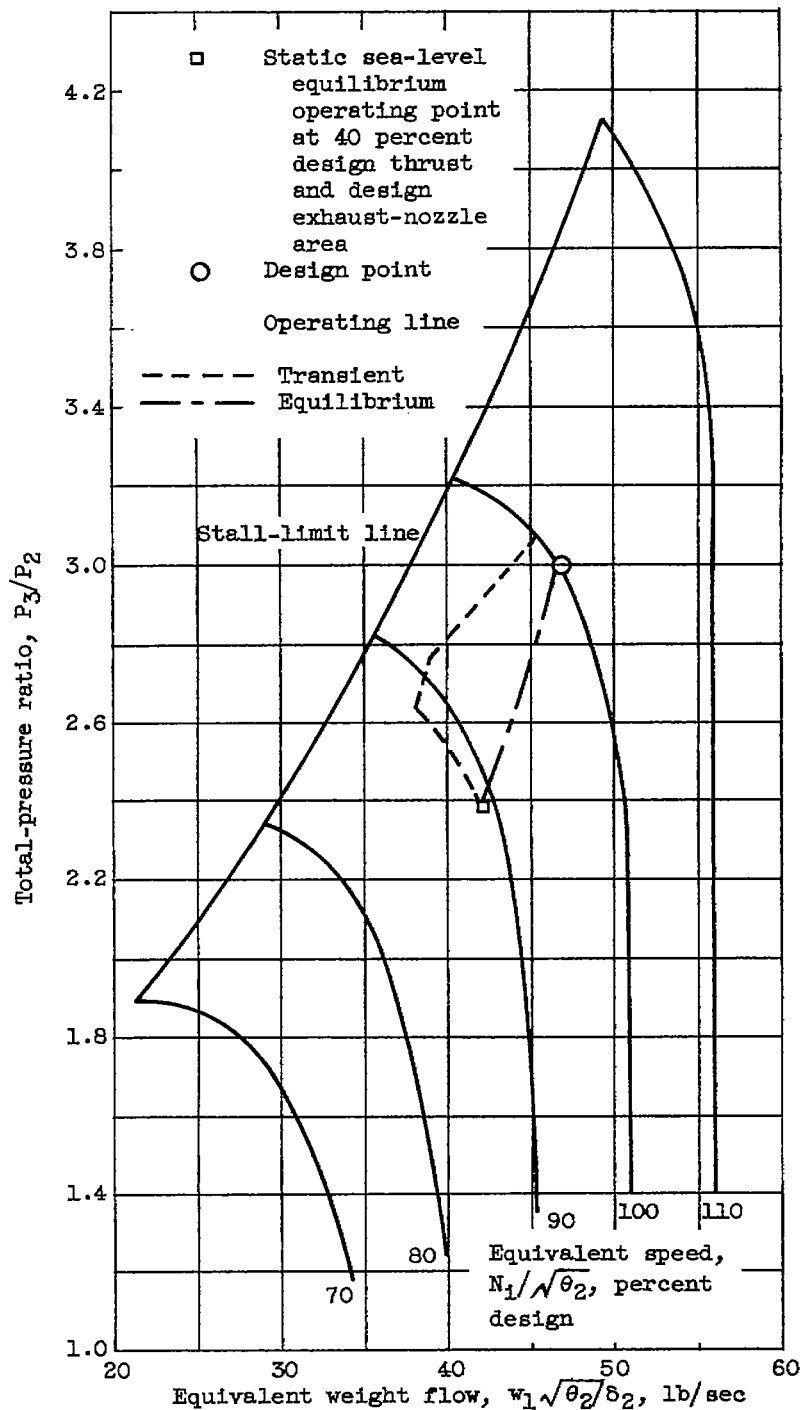

(a) Engine 26.

Figure 3. - Outer-compressor component performance maps.

(b) Engine 34.

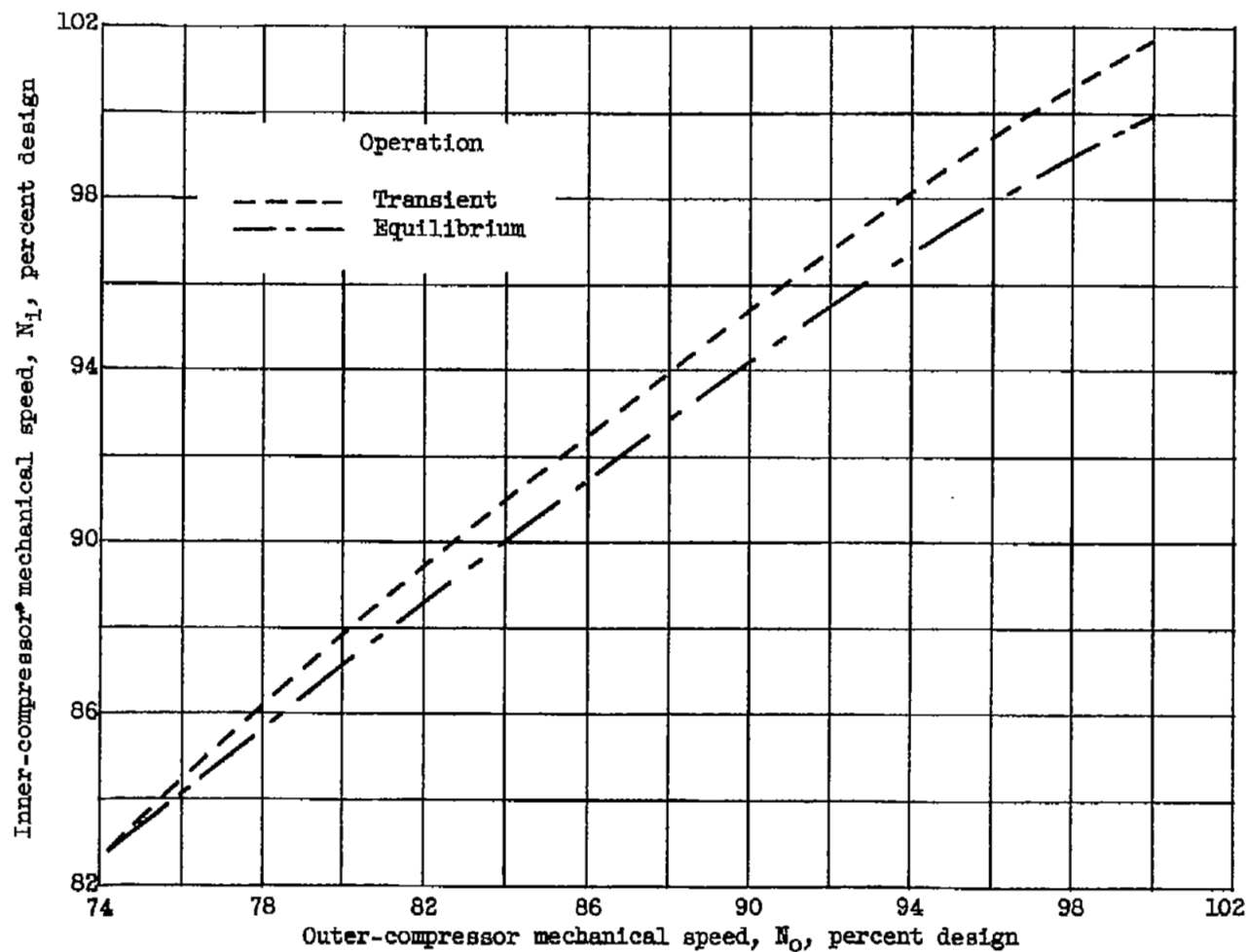Figure 3. - Continued. Outer-compressor component performance maps.

3993

CY-3

The figure plots Total-pressure ratio, P_2/P_1, (vertical axis, ranging 1 to 6) against Equivalent weight flow, $w_1\sqrt{\theta_1}/\delta_1$, lb/sec (horizontal axis, ranging 60 to 180).

Legend:
- ☐ Static sea-level equilibrium operating point at 40 percent design thrust and design exhaust-nozzle area
- ○ Design point

Operating line
- – – – – Transient
- — · — Equilibrium

Stall-limit line

Equivalent speed, $N_0/\sqrt{\theta_1}$, percent design: 70, 80, 90, 100, 110

(c) Engine 43.

Figure 3. - Concluded. Outer-compressor component performance maps.

(a) Engine 26.

Figure 4. - Inner-compressor component performance maps.

CY-3 back   3993
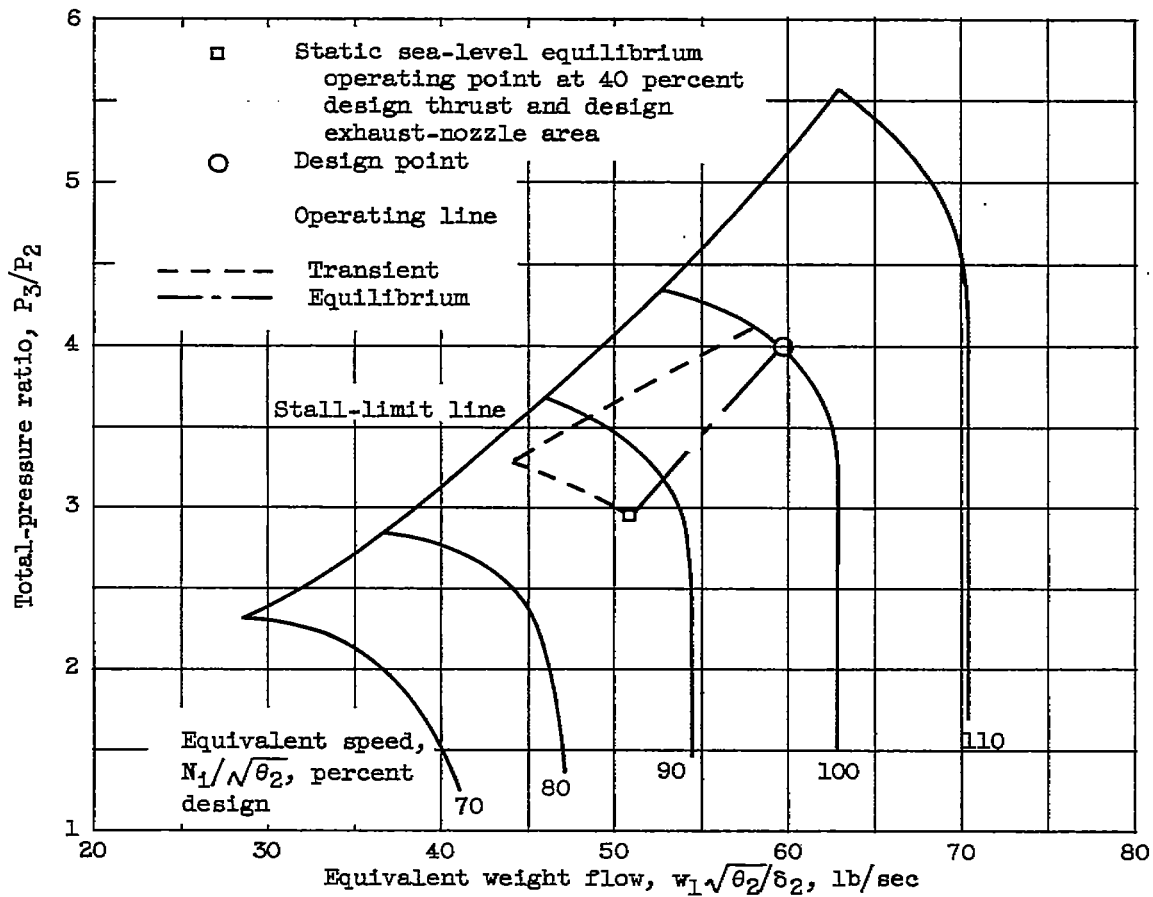
(b) Engine 34.

Figure 4. - Continued. Inner-compressor component performance maps.

(c) Engine 43.

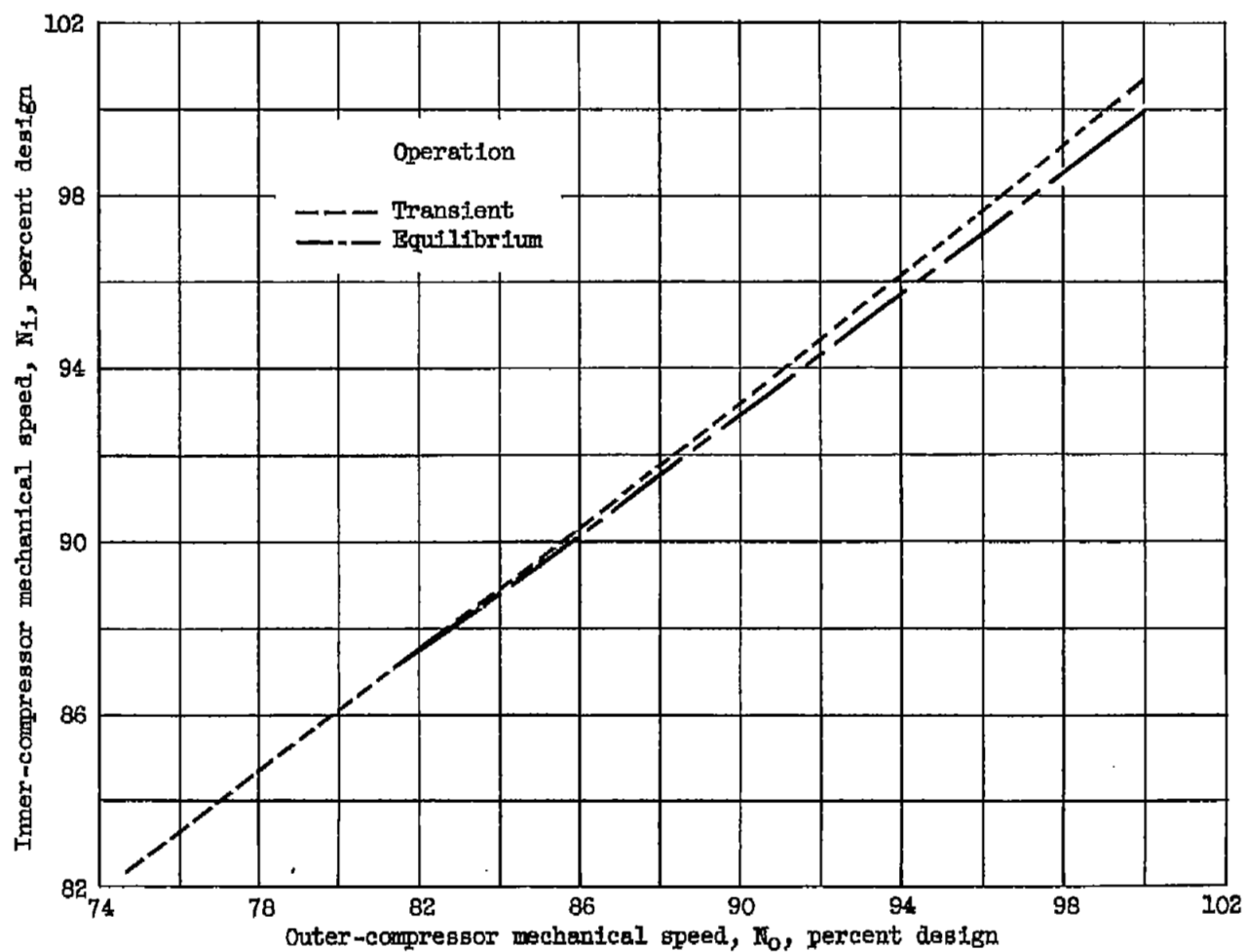Figure 4. - Concluded. Inner-compressor component
performance maps.
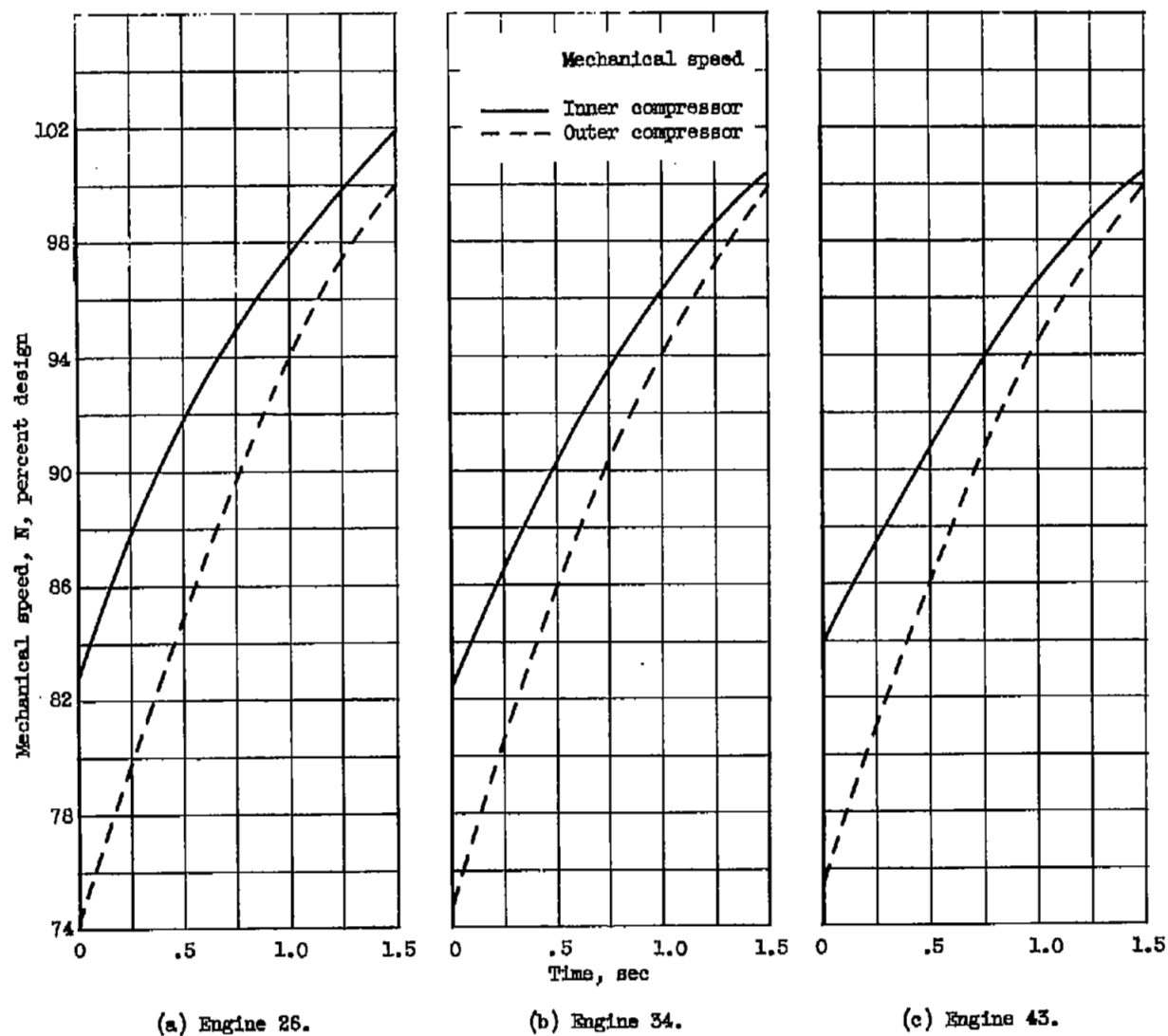
Figure 5. - Speed variation with time of inner and outer compressor for engines operating at static sea-level conditions.
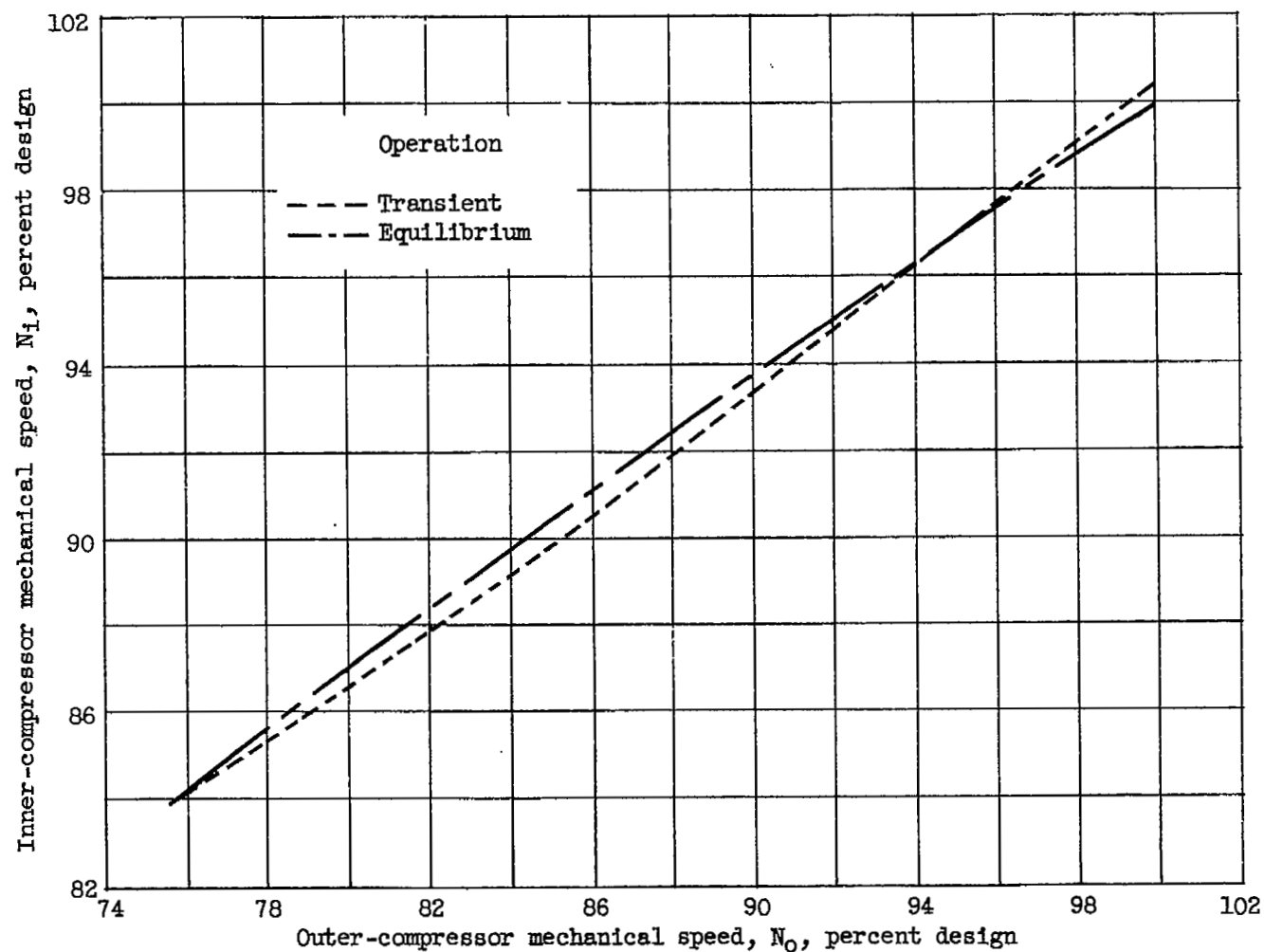
(a) Engine 26.

(b) Engine 34.

(c) Engine 43.

(a) Engine 26.

Figure 6. - Variation of inner- with outer-compressor mechanical speeds during acceleration.

(b) Engine 34.

Figure 6. – Continued. Variation of inner- with outer-compressor mechanical speeds during acceleration.

(c) Engine 43.

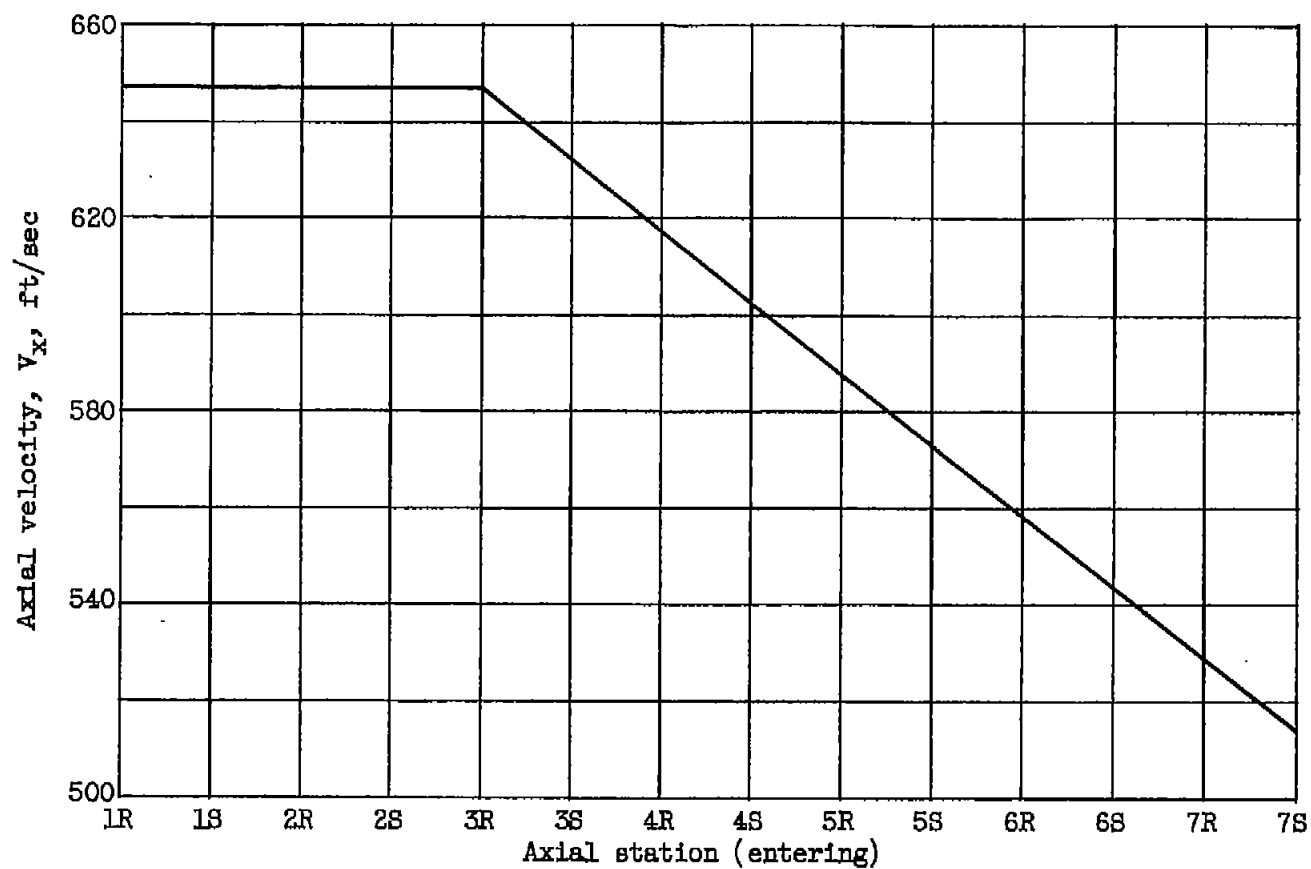Figure 6. - Concluded. Variation of inner- with outer-compressor mechanical speeds during acceleration.

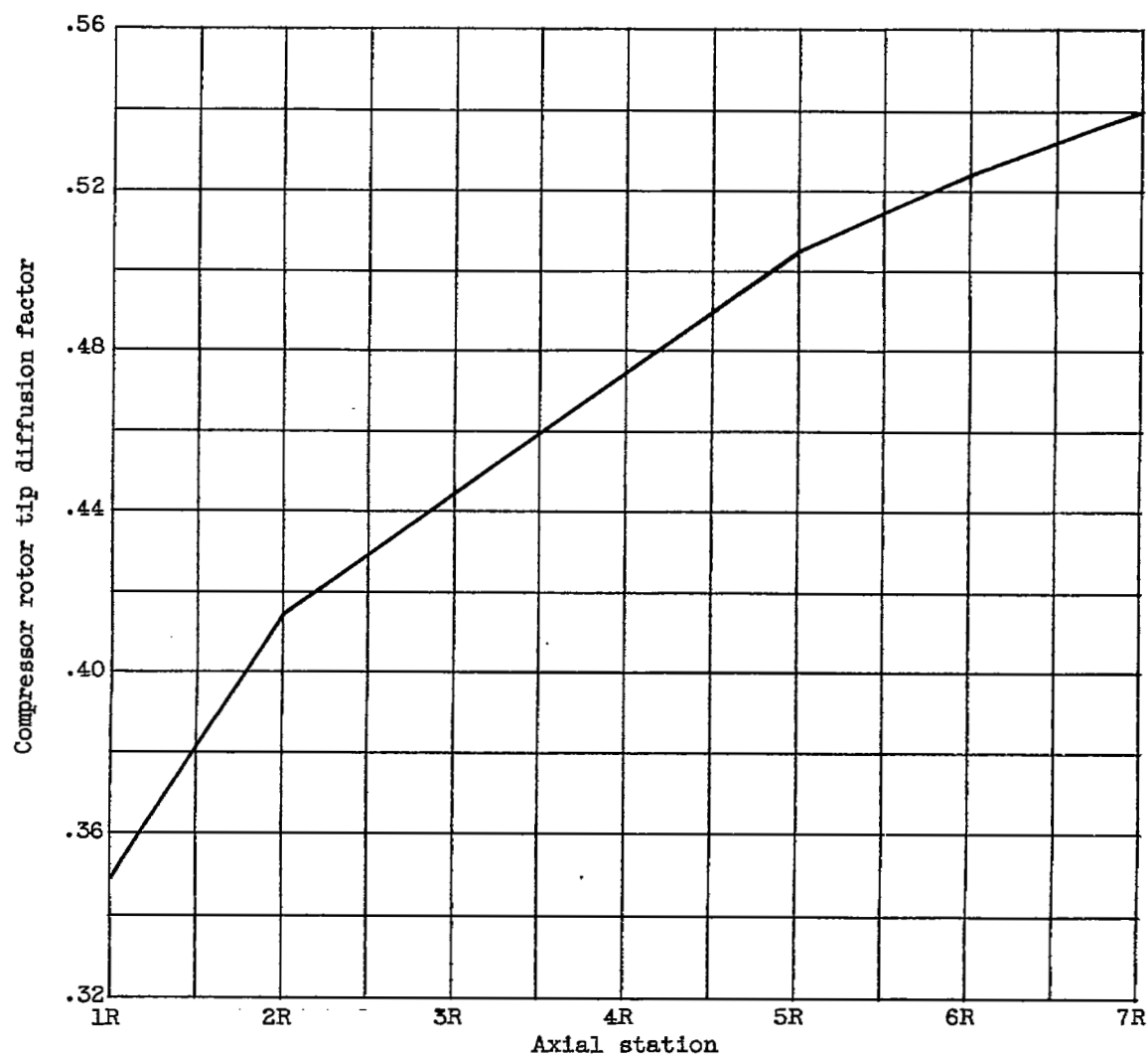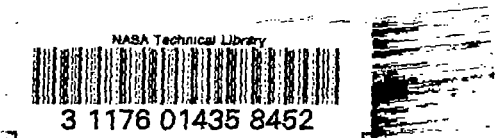Figure 7. - Variation of axial velocity with compressor axial station.

NACA RM E56D13

Figure 8. - Variation of compressor rotor tip diffusion factor with axial station.